SANDIA REPORT

SAND97–0295 • UC–704
Unlimited Release
Printed February 1997

Final Report on LDRD Project: In Situ Determination of Composition and Strain During MBE

E. Chason, J.A. Floro, J. Reno, J. Klem

Prepared by
Sandia National Laboratories
Albuquerque, New Mexico 87185 and Livermore, California 94550
for the United States Department of Energy
under Contract DE-AC04-94AL85000

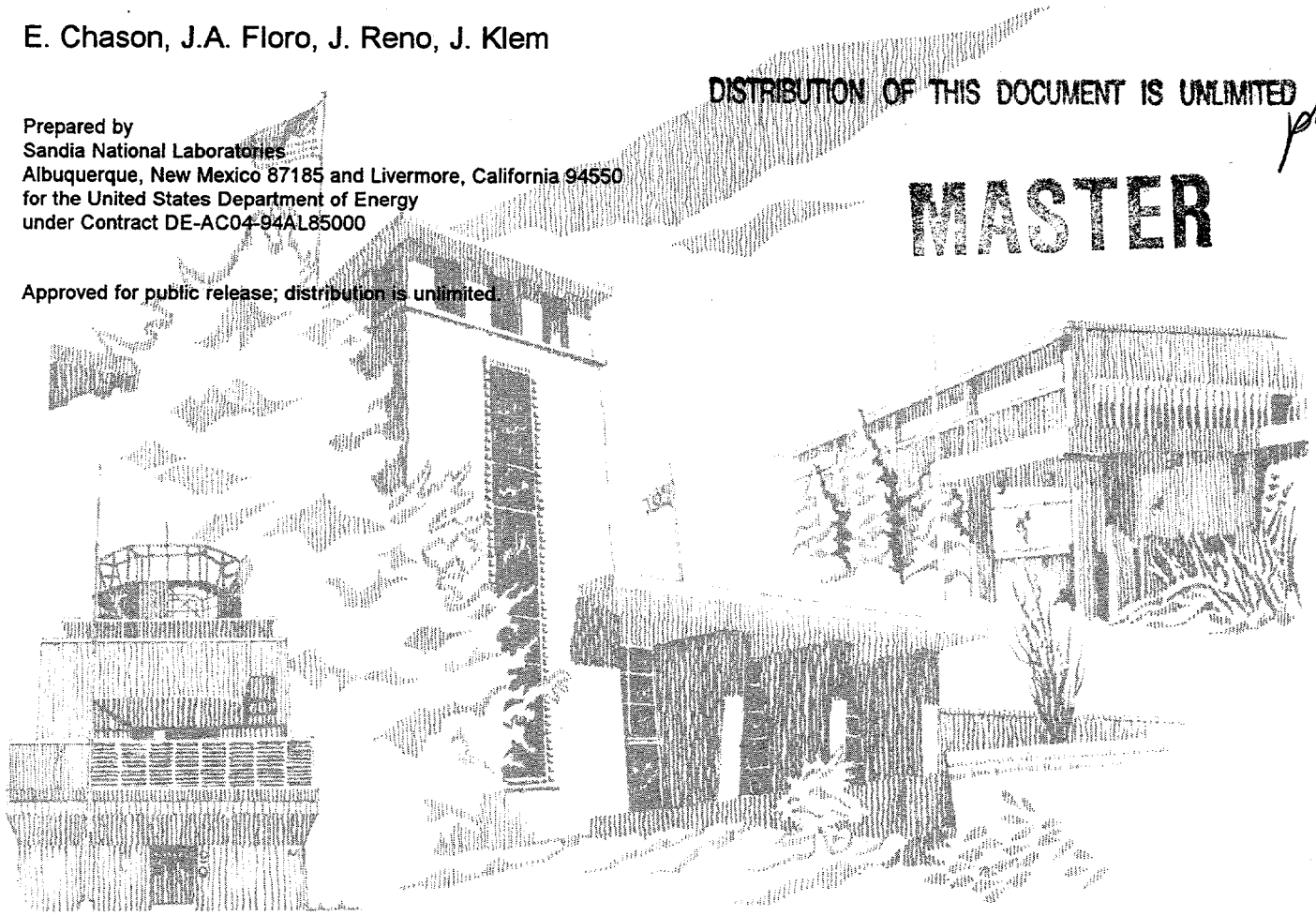

Issued by Sandia National Laboratories, operated for the United States Department of Energy by Sandia Corporation.

Available to DOE and DOE contractors from
Office of Scientific and Technical Information
P.O. Box 62
Oak Ridge, TN 37831

Prices available from (615) 576-8401, FTS 626-8401

Available to the public from
National Technical Information Service
U.S. Department of Commerce
5285 Port Royal Rd
Springfield, VA 22161

NTIS price codes
Printed copy: A03
Microfiche copy: A01

SAND97-0295
Unlimited Release
Printed February 1997

Distribution
Category UC-704

Final Report on LDRD Project: *In Situ* Determination of Composition and Strain during MBE

E. Chason and J. A. Floro
Nanostructure and Semiconductor Physics Department

J. Reno
Semiconductor Material and Device Sciences Department

J. Klem
Compound Semiconductor Materials and Processes Department

Sandia National Laboratories
P.O. Box 5800
Albuquerque, NM 87185-1415

Abstract

Molecular Beam Epitaxy (MBE) of semiconductor heterostructures for advanced electronic and opto-electronic devices requires precise control of the surface composition and strain. The development of advanced in situ diagnostics for real-time monitoring and process control of strain and composition would enhance the yield, reliability and process flexibility of material grown by MBE and benefit leading-edge programs in microelectronics and photonics. We have developed a real-time laser-based technique to measure the evolution of stress in epitaxial films during growth by monitoring the change in the wafer curvature.

Research has focused on the evolution of stress during the epitaxial growth of Si_xGe_{1-x} alloys on Si(001) substrates. Initial studies have observed the onset and kinetics of strain relaxation during the growth of heteroepitaxial layers. The technique has also been used to measure the segregation of Ge to the surface during alloy growth with monolayer sensitivity, an order of magnitude better resolution than post-growth characterization. In addition, creation of a 2-dimensional array of parallel beams allows rapid surface profiling of the film stress that can be used to monitor process uniformity.

Intentionally Left Blank

Table of Contents

Intentionally Left Blank

Final Report on LDRD Project:
In Situ Determination of Composition and Strain during MBE

Case number: 3539.320

Project Manager: S/T/ Picraux, 1112

Principal Investigators: E. Chason, 1112 , J.A. Floro, 1112, J. Reno, 1113, J. Klem, 1311

Abstract

Molecular Beam Epitaxy (MBE) of semiconductor heterostructures for advanced electronic and opto-electronic devices requires precise control of the surface composition and strain. The development of advanced in situ diagnostics for real-time monitoring and process control of strain and composition would enhance the yield, reliability and process flexibility of material grown by MBE and benefit leading-edge programs in microelectronics and photonics. We have developed a real-time laser-based technique to measure the evolution of stress in epitaxial films during growth by monitoring the change in the wafer curvature.

Research has focused on the evolution of stress during the epitaxial growth of Si_xGe_{1-x} alloys on Si(001) substrates. Initial studies have observed the onset and kinetics of strain relaxation during the growth of heteroepitaxial layers. The technique has also been used to measure the segregation of Ge to the surface during alloy growth with monolayer sensitivity, an order of magnitude better resolution than post-growth characterization. In addition, creation of a 2-dimensional array of parallel beams allows rapid surface profiling of the film stress that can be used to monitor process uniformity.

Accomplishments

The technique is based on measuring the curvature of the substrate induced by the stress in the film. An array of parallel laser beams is created from a single beam using a highly reflective optical element called an etalon. This array is reflected from the thin film surface, and deflections of the beams (as measured by a CCD camera) are used to determine the curvature of the substrate, which is proportional to the product of the film stress and the film thickness. The multi-beam approach provides reduced sensitivity to vibration and greater ease of operation than prior techniques. The system is capable of measuring radii of curvature greater than 4 kM in situ, which is sufficient to measure the stress resulting from 0.1 monolayers of Ge on a Si(001) surface. By using a pair of etalons rotated orthogonally, a two-dimensional array of parallel laser beams can be produced. Measuring the deflections of these beams enables a full surface profile of the stress to be obtained rapidly, with no beam scanning. This rapid profiling capability can be used to monitor process uniformity in real time.

The laser technique has been used to measure the evolution of stress during the deposition of SiGe films on Si(001) substrates. In the first sets of experiments, the kinetics of relaxation of strained layers were determined. Previous approaches to measure these kinetics required many

samples to be grown and analyzed after growth. Using the laser curvature technique, the critical thickness for dislocation formation could be determined from a single growth run for each growth temperature. In addition, the subsequent relaxation kinetics after the initial dislocation nucleation were measured.

For a pseudomorphically strained heterolayer (no dislocations), the strain in the layer is constant. Therefore, the curvature, which is proportional to the product of the film strain and the thickness, should be proportional to the film thickness. However, during the growth of SiGe alloys on Si(001), we observed an initial transient before the eventual linear increase in the curvature. By analysis of the stress evolution, we determined that this transient is due to the initial segregation of Ge to the surface during the early stages of growth. This data was then used to determine the composition profiles of the alloy layers with monolayer sensitivity, more than an order of magnitude better than can be obtained by post-growth characterization techniques.

List of Publications, Presentations, and Patent Applications

Publications

1. J.A. Floro, E. Chason, and S.R. Lee, Real-Time Measurements of Epilayer Strain Using a Simplified Wafer Curvature Technique, Mat. Res. Soc. Symp. Proc., 1996.

2. E. Chason and J.A. Floro, Measurements of Stress Evolution during Thin Film Deposition, Mat. Res. Soc. Symp. Proc., 1996.

3. J.A. Floro and E. Chason, Ge Segregation Profiles Determined by Real Time Surface Stress Measurements during SiGe MBE, Appl. Phys. Lett., 1996.

Presentations

1. J.A. Floro, E. Chason, and S.R. Lee, Real-Time Measurements of Epilayer Strain Using a Simplified Wafer Curvature Technique, Mat. Res. Soc., Nov. 1995, Boston, MA.

2. E. Chason and J.A. Floro, Measurements of Stress Evolution during Thin Film Deposition, Mat. Res. Soc. April 1996, San Francisco, CA.

3. J.A. Floro and E. Chason, Mat. Res. Soc., Apr. 1996, San Francisco, CA.

4. J.A. Floro and E. Chason, Real Time Measurements of Strain Evolution during Thin Film Heteroepitaxy, Mat. Res. Soc., Dec. 1996, Boston, MA (invited).

Patent Applications

1. E. Chason, J.A. Floro, M.B. Sinclair, and C.H. Seager, Measurement of the Curvature of a Surface Using Parallel Beams, S-85,031, SD-5750, filing date Nov. 25, 1996.

Intentionally Left Blank

REAL TIME MEASUREMENT OF EPILAYER STRAIN USING A SIMPLIFIED WAFER CURVATURE TECHNIQUE

J. A. FLORO, E. CHASON, and S. R. LEE
Sandia National Laboratories, Albuquerque, NM, 87185-1415, jafloro@sandia.gov

ABSTRACT

We describe a technique for measuring thin film stress using wafer curvature that is robust, compact, easy to setup, and sufficiently sensitive to serve as a routine diagnostic of semiconductor epilayer strain in real time during MBE or CVD growth. We demonstrate, using growth of SiGe alloys on Si, that the critical thickness for misfit dislocation can clearly be resolved, and that the subsequent strain relaxation kinetics during growth or post-growth annealing are readily obtained.

INTRODUCTION

The bandstructure and transport properties of electronic and optoelectronic materials can be significantly modified by the presence of coherency strain associated with the pseudomorphic heteroepitaxial growth of the material on a substrate with a different lattice parameter. Device designers take advantage of this effect in the fabrication of novel high performance devices using strained alloy or compound semiconductor thin films typically grown by molecular beam epitaxy (MBE) or by chemical vapor deposition (CVD). Monitoring and controlling the degree of strain (which is determined by the epilayer composition, the substrate lattice parameter, and the degree of strain relaxation) is a significant challenge to the epilayer grower. An in situ diagnostic that can determine the strain state in real time during growth or subsequent thermal annealing would clearly be of great utility, especially if the diagnostic can operate in the CVD environment as well as in the MBE environment.

In this paper we describe a technique for epilayer strain determination. We measure the curvature of the underlying substrate to determine the stress, and therefore the strain, of the epilayer in real time during growth. The technique uses a laser as a probe, and is thus compatible with both the CVD and MBE environments (as long as optical access to the substrate is available). While curvature-based stress measurements have found wide application in the broader thin films community, relatively little use of this approach has been made within the semiconductor epilayer growth community. We have designed our particular variation of the curvature technique with robustness, compactness, and ease of use for the grower as our primary goals. We first briefly discuss the relevant background and prior art in this area, and then describe our approach. After examining the strain sensitivity of this technique, we present an example of its capabilities using SiGe MBE growth as a demonstration.

An alternative technique applicable to MBE growth is Reflection High Energy Electron Diffraction (RHEED). RHEED measures the surface lattice parameter of a growing epilayer, which is often the quantity of greatest interest, especially when a compositionally graded, partially relaxed buffer layer is being grown. Several measurements of the surface lattice parameter during III-V epilayer growth have been presented [1,2]. The advantages of the laser curvature technique are: (1) useful in the typical high pressure CVD environment; (2) insensitivity to stray electric and magnetic fields, making the technique easier to use when high-current sample heaters are in use, or when electron-beam evaporators are employed as deposition sources (e.g., for Si deposition); and (3) routine use is simple with no knowledge of diffraction required.

BACKGROUND AND PRIOR ART

A biaxially strained thin film rigidly attached to a much thicker substrate induces a curvature $\kappa = 1/R$, where R is the radius of curvature, given by [3,4]

$$\kappa - \kappa_0 = \frac{M_f h_f \varepsilon}{6 M_s h_s^2}, \qquad (1)$$

where ε is the biaxial strain, $M_{f,s}$ are the film, substrate biaxial moduli, and $h_{f,s}$ are the film, substrate thicknesses. κ_0 is the initial curvature of the substrate prior to film growth. Curvature resolution is clearly enhanced by reducing substrate thickness. Note that it is the film stress $\sigma = M_f \varepsilon$ that is determined directly from a curvature measurement. Determining film strain requires knowledge of the biaxial modulus of the film.

There are many ways in which to measure the curvature of a substrate. We focus here on the deflection of a laser beam incident on multiple points on the sample. The deflection arises from the spatially varying surface normal of the film/substrate combination due to its stress-imposed curvature. As discussed below, we monitor the deflection of multiple parallel laser beams using a CCD array detector. This is in contrast to the laser scanning techniques, where a single laser beam is moved point-to-point across a sample, typically through use of a rotating mirror [5]. The laser is located exactly at the focal plane of a long focal length lens, thus converting the angular scan of the mirror into a linear scan across the sample. A position sensitive detector (PSD) is also located at the focal plane of the same lens. In this configuration, the scanned beam will arrive at the same point on the PSD if the wafer is flat. A uniformly curved wafer produces a constant deflection during scanning that is proportional to the curvature. This technique is sensitive and is sufficiently rapid to perform real-time measurements. It has been applied, for example, to the measurement of strain relaxation kinetics of SiGe alloys on Si during growth [6] and furnace annealing [7]. The primary drawbacks to this technique are associated with matters of operational convenience, in particular the need for precise alignment of the laser and PSD relative to the lens, and the use of a rotating mirror. An alternative approach to laser scanning is to use two stationary laser beams (e.g., produced by a single laser and a beamsplitter) and measure their separation using quadrant photodiodes [8]. The change in beam spacing with time is again directly proportional to the wafer curvature. The technique is simple, sensitive, and robust. The only drawback is that only two points are sampled. In the next section we describe two modifications to this approach that further refine the ease of use and setup.

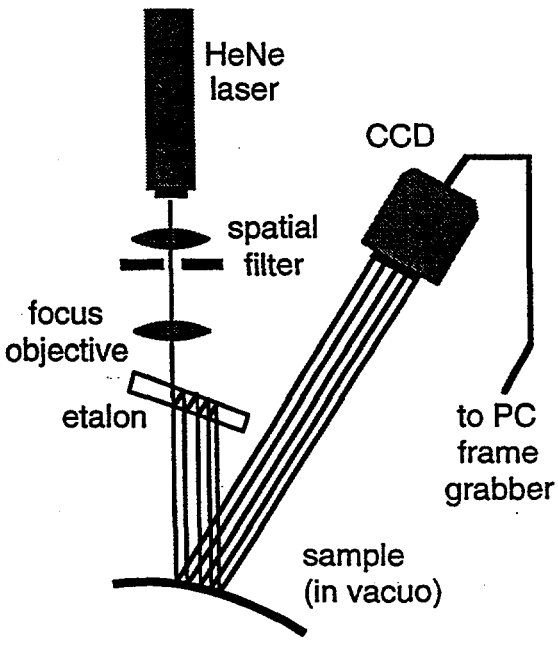

Figure 1. Schematic setup of the curvature measurement technique.

THE TECHNIQUE

Our generic setup is shown in Fig. 1. A single polarized HeNe laser beam is converted into multiple parallel beams through use of a highly reflective etalon. The output beam spacing is determined by the angle between the laser beam axis and the surface normal of the etalon. We typically employ five - a practical limit on the number of beams arises from the reduced intensity of each subsequent beam. For an etalon with surfaces of reflectivity R, $I_n/I_1 = R^{2(n-1)}$, where I_n is the

intensity of the n^{th} transmitted beam and I_1 is the intensity of the first transmitted beam. In the experiments presented here, $R = 0.9$ and hence $I_5/I_1 = 0.43$. Higher reflectivity etalons reduce the relative intensity loss I_5/I_1 at the expense of also reducing the absolute intensity.

After reflection off the sample, the beams are detected on a Peltier-cooled CCD camera. The only other optics employed are a spatial filter (lens and pinhole) to "clean up" the beam profile, and a focusing objective that focuses the beam on the camera. Additional attenuators may be necessary to reduce the beam intensity to avoid saturating the CCD. The use of a CCD permits simple detection of more than two beams. In addition, the CCD camera allows for easy focusing of the beams, which is important for obtaining maximum sensitivity. Finally, commercial acquisition hardware and software are readily available [9]. The primary drawbacks are the "digitization" of the analog beam distribution, which reduces spatial resolution, and the limited size of the CCD array, which limits the maximum sample region to be probed.

In order to determine the substrate curvature we measure the spacing between each adjacent beams D. Curvature is determined from the differential spacing $\Delta D/D_0$ by

$$\frac{\Delta D}{D_0} = \frac{2L\kappa}{\cos\alpha}, \qquad (2)$$

where $D_0 = D(t=0)$, $\Delta D = D(t) - D_0$, L is the length from sample to CCD array, and α is the angle of incidence on the sample ($\alpha = 0°$ for normal incidence). Spatially resolved curvature measurements are obtained by tracking each differential spacing independently. For the purposes of this paper we spatially average over all the measured spacings to arrive at one mean differential spacing $\langle\Delta D/D_0\rangle$ and thus one average curvature.

The laser beam positions on the CCD array are determined through use of PC-based image acquisition software and hardware originally developed for RHEED applications [9]. A "window" is placed around each laser spot on the CCD image. Periodically the frame grabber acquires the full image and determines the centroid of the intensity distribution within each window. The row and column position of the centroid is then written to disk. The software allows each window to track the centroid, preventing loss of accuracy due to curvature- or drift-induced beam motion. Currently the software permits real-time data acquisition, but does not analyze or display quantities such as the differential spacing or the strain in real time. Thus, after growth the time-varying centroid positions are differenced to get the spacings D(t).

One requirement in order to accurately determine the strain from measurements of the substrate curvature is that the sample be mounted such that the bending of the substrate is unconstrained. We have used a "cage" about the perimeter of the sample that allows the sample full bending freedom, allows for RHEED access, and permits backside radiative heating.

SENSITIVITY

In order to determine the sensitivity and resolution of the setup, we measure the mean differential spacing on a static (no growth) 2" diameter Si wafer, 0.28 mm thick, as a function of time. In this case the mean differential spacing fluctuates about zero. The maximum resolvable radius of curvature R_{max} is then determined by taking $\langle\Delta D/D_0\rangle$ to be twice the standard deviation of the fluctuations in the signal. The laser apparatus is mounted on a turbopumped MBE (with no special provisions for vibration reduction or isolation) with a relatively compact sample-to-CCD distance of L = 66 cm and $\alpha = 3°$. We find $\langle\Delta D/D_0\rangle_{static} = 0.0004$, which, from equation 2, gives $R_{max} = 1.7$ km. Using equation (1) we can relate R_{max} to the minimum resolvable thickness of an epilayer with a strain ε. For demonstration purposes we will calculate this using values appropriate to the SiGe/Si experiments to be described in the next section. Taking $h_s = 0.28$mm, $M_{Si} = 180.4$ GPa, and $M_{Ge} = 168.9$ GPa (and interpolating the alloy modulus using the rule of mixtures), h_f^{min} vs. ε is calculated and plotted in Fig. 2. As an example of the interpretation of this curve, we see

that for a film with 1% strain ($Si_{75}Ge_{25}$), 6 monolayers of film are detectable, and for a film with 4% strain, 2 monolayers are detectable. Conversely, for a film 200 Å thick, strains less than 0.1% can be resolved. For comparison, we also plot in Fig. 2 the equilibrium critical thickness [10] for misfit dislocation formation. We find that the critical thickness curve lies everywhere above the h_f^{min} curve, implying that for any $Si_{(1-x)}Ge_x$ composition we have sufficient resolution to detect the equilibrium critical thickness. We may generalize beyond SiGe by considering both the specific form of the epitaxial critical thickness h_c (we use here the form given by Freund [11]) and the minimum resolvable epilayer thickness h_{min} from the curvature measurement:

$$h_c = \frac{b\left(1-\cos^2\beta\right)\ln\left(2h_c/r_0\right)}{8\pi(1+\nu)\sin\alpha\sin\beta\,\varepsilon}, \qquad h_{min} = \frac{M_s h_s^2}{6M_f R_{max}\varepsilon}, \tag{3a), (3b}$$

where b is the Burgers vector, ν is Poisson's ratio, $\alpha = 54.74°$ and $\beta = 60°$ for (001) epitaxy, r_0 is the dislocation core cutoff width, and all other quantities are as defined previously. In order to detect the critical thickness by our technique, we must have $h_c/h_{min} \geq 1$. If we take the ratio of equations 3a and 3b, and substitute $\nu = 1/3$, the values of α and β given above, and we approximate $h_c = 10r_0$ in the logarithmic term (since we are concerned with small critical thicknesses), we arrive at

$$\frac{bR_{max}}{h_s^2}\left(\frac{M_f}{M_s}\right) \geq 1.44, \tag{4}$$

If we further take $M_f = M_s$, $R_{max} = 1.7$ km, and b = 2 Å, and solve for the substrate thickness, we get $h_s < 0.49$ mm in order to resolve the critical thickness for a typical heteroepitaxial semiconductor system. If thicker substrates are used, then the sensitivity must be increased. This may be attained by increasing the sample-to-CCD distance L (equation (2)), although the actual gain in sensitivity depends on the source of the noise.

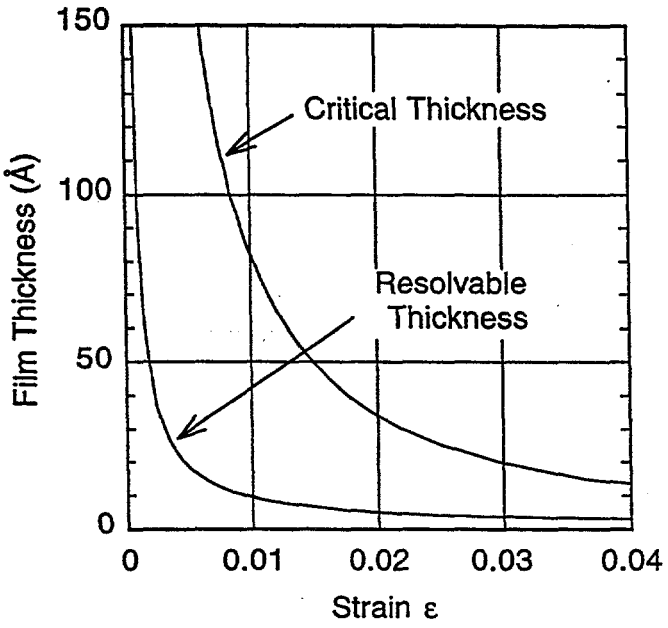

Figure 2. Thickness/strain sensitivity curve for SiGe on 0.28 mm Si (001) substrates. Also plotted is the equilibrium critical thickness curve for SiGe/Si.

HETEROEPITAXIAL GROWTH OF SiGe

During growth, the differential spacing is related to the strain and film thickness by

$$\frac{\Delta D}{D_0} = F\varepsilon(t)h_f, \qquad F = \frac{12LM_f}{M_f h_s^2 \cos\alpha}, \tag{5a), (5b}$$

where we recognize that the strain can be time dependent during the relaxation regime. Prior to relaxation the strain is constant and the differential spacing will vary linearly with thickness. Thus, unlike RHEED, we obtain a positive determination that a coherently strained layer is growing.

In order to demonstrate the real time capabilities of the technique, we grow uniform SiGe alloys of composition 29% Ge (1.2% strain), and total deposition rate 0.6 Å/s. Composition is verified by x-ray diffraction measurements and the final thicknesses by RBS. The substrates consist of sections of 2" diameter Si (001) wafers, 0.28 mm thick. The substrates are chemically cleaned, leaving a final weakly-bound oxide passivated surface. The oxide is desorbed in situ at 830°C and a 1200Å Si buffer is grown at 700°C. Surface quality and reconstruction is monitored by RHEED. A smooth, 2x1 reconstructed surface serves as the starting point for alloy growth. The substrate is equilibrated at the growth temperature (measured by pyrometer) for at least one hour. Deposition is accomplished with electron beam evaporators. Prior to opening the shutters to expose the substrate to the growth fluxes, the laser spot positions are measured for 100 seconds to determine the initial spacings D_0. The laser enters and exits through a standard glass viewport.

In Fig. 3 we show the mean differential spacing as a function of film thickness for alloys grown at three temperatures. These measurements were carried out to much larger thicknesses, but we concentrate on the early stages of growth to highlight the deviation from linearity. For all three layers the mean differential spacing initially varies linearly with thickness, indicating fully coherent growth. All three curves eventually become sublinear, with the deviation occurring at greater thicknesses for lower growth temperatures. The points at which deviation occurs define the kinetically limited critical thicknesses. For the film grown at 650°C, the critical thickness is exactly the equilibrium value predicted by equation (3a). Thus we are easily able to map out the critical thickness as a function of growth temperature, and to verify the equilibrium h_c by growing at sufficiently high temperature.

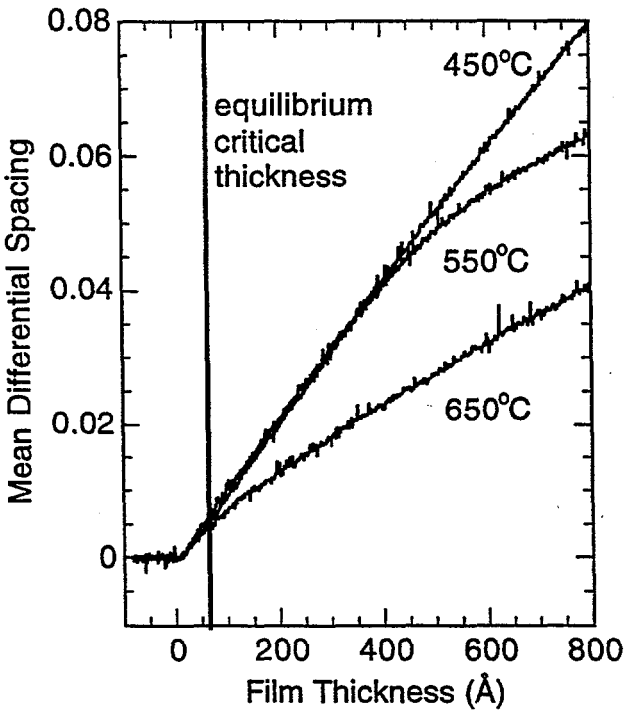

Figure 3. Mean differential spacing vs. film thickness for $Si_{71}Ge_{29}$ epilayers during growth on Si (001), for three growth temperatures.

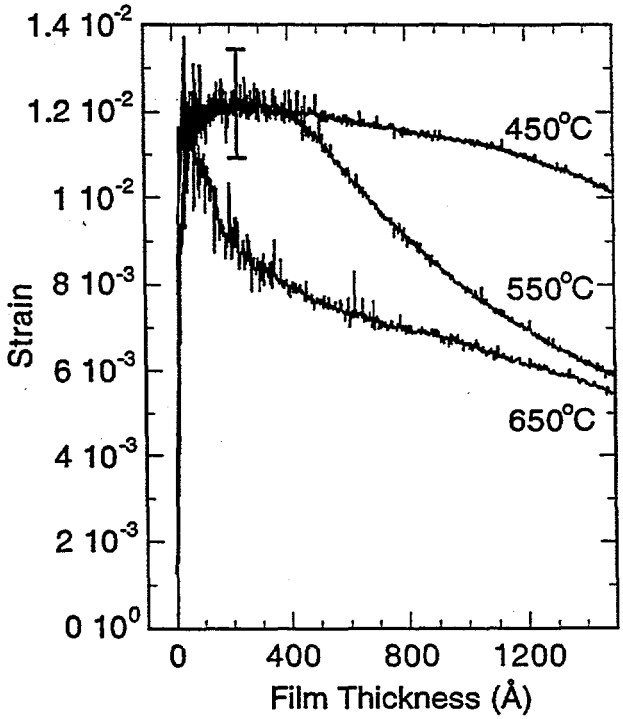

Figure 4. Strain in $Si_{71}Ge_{29}$ epilayers during growth on Si (001), for three growth temperatures.

In Fig. 4 we plot strain vs. film thickness for the same three films shown in Fig. 3. The strain is obtained by inverting equation (5a). The plateau regions at low thicknesses correspond to the coherent regime. Past the critical thickness, an S-shaped relaxation profile representing the nucleation and glide of misfit dislocations is observed. The final degree of relaxation in the films has also been verified ex situ by x-ray diffraction. We note that the accuracy in the absolute determination of the strain is limited by the accuracy to which the parameter F in equation (5) is known. This is typically dominated by error in substrate thickness measurement. The error bar in Fig. 4 represents a $\pm$ 5 μm error in substrate thickness.

Finally we note that the mean differential spacing is the most sensitive parameter for determining the critical thickness, while the strain vs. thickness (or time) is best suited for evaluation relaxation kinetics.

CONCLUSIONS

We have developed a technique for measuring substrate curvature, and thus film strain, that is robust, compact, easy to set up, and sufficiently sensitive to routinely evaluate epilayer critical thicknesses and strain relaxation kinetics. The technique can be used in both MBE and CVD growth environments, as long as optical access is available and the substrate is free to bend. The technique has been designed as an in situ, real time diagnostic of semiconductor heteroepitaxy, but can also be used to determine strain during growth of polycrystalline and amorphous materials (unlike RHEED). The curvature technique only determines an average strain over the thickness of the epilayer, which may be a limitation for graded layers or multilayers. Nonetheless, the simplicity and sensitivity of this approach should make it a useful diagnostic in a variety of growth situations.

ACKNOWLEDGMENTS

Our thanks to Mike Sinclair and Carl Seager for optics advice, and to Jay Penn for assistance with the setup and MBE growth. We are grateful to Darryl Barlett of k-Space Associates for timely modifications to his software. This work was performed at Sandia National Labs and supported by the U. S. Department of Energy under contract DE-AC04-94AL85000.

REFERENCES

1. J. Mirecki-Millunchick and S. A. Barnett, Appl. Phys. Lett. **65** 1136 (1994)
2. G. J. Whaley and P. I. Cohen, Appl. Phys. Lett. **57**, 144 (1990).
3. G. G. Stoney, Proc. R. Soc. London Ser. A **82**, 172 (1909).
4. P. H. Townsend, D. M. Barnett, and T. A. Brunner, J. Appl. Phys. **62**, 4438 (1987).
5. Paul A. Flinn, Donald S. Gardner, and William D. Nix, IEEE Trans. Electron Devices **ED-34**, 689 (1987).
6. Veronique T. Gillard and William D. Nix, Zeitschrift fur Metallkunde **84**, 874 (1993).
7. C. A. Volkert, E. A. Fitzgerald, R. Hull, Y. X. Hie, and Y. J. Mi, J. Elec. Mater. **20**, 833 (1991).
8. A. J. Schell-Sorokin and R. M. Tromp, Phys. Rev. Lett. **64**, 1039 (1990).
9. k-Space Associates, Inc., 2231 Stone Drive, Ann Arbor, MI 48105.
10. L. B. Freund, J. Mech. Phys. Solids **38**, 657 (1990).

MEASUREMENTS OF STRESS EVOLUTION DURING THIN FILM DEPOSITION

E. CHASON AND J.A. FLORO
Sandia National Laboratories, Albuquerque, NM 87185-1415

ABSTRACT

We have developed a technique for measuring thin film stress during growth by monitoring the wafer curvature. By measuring the deflection of multiple parallel laser beams with a CCD detector, the sensitivity to vibration is reduced and a radius of curvature limit of 4 km has been obtained in situ. This technique also enables us to obtain a 2-dimensional profile of the surface curvature from the simultaneous reflection of a rectangular array of beams. Results from the growth of SiGe alloy films are presented to demonstrate the unique information that can be obtained during growth.

INTRODUCTION

Understanding and controlling stress in thin films is critical for tailoring their optical, electronic and mechanical properties. Precise control of layer strain is required for the production of compound semiconductor heterostructure devices, and stress induced process can lead to the failure of interconnects and delamination of films. In general, most studies of thin film stress are performed after the films are grown. In this work, we discuss a new approach for measuring stress evolution *in situ* during the growth of thin films. We present results from experiments during epitaxial growth of SiGe alloy layers on Si(001) substrates with particular emphasis on the new information about the growth process that can be obtained from real time stress measurements.

WAFER CURVATURE MEASUREMENTS USING LASER BEAMS

A thin film under stress on a substrate will lead to bending of the substrate [1]. The radius of curvature of the substrate that results will be due to the balancing of the external bending moment applied and the bending moment of the curved substrate. The resulting curvature can be detected by the deflection of a beam of light incident upon the sample. If the substrate is flat, then the angle of reflection will be the same anywhere on the surface. However if the substrate is curved, then the reflection angle will change as the beam is moved across the surface.

Various experimental approaches have been devised to measure the curvature of the surface. The scanning mirror technique [2,3,4,5] uses a rotating mirror and lens to scan the laser beam across the sample without changing the angle of incidence. A position sensitive detector measures the deflection of the beam as it is scanned. Alternatively, a beam splitter has been used [6,7,8] to produce two parallel beams whose deflections are measured independently with position sensitive detectors.

We have developed a variation of this technique with some features that simplify its use as an in situ diagnostic during growth. The experimental setup is shown in figure 1. An etalon that has been coated with highly reflective layers on both sides is placed at an angle to the laser beam. The non-normal incidence leads to multiple internal reflections inside the etalon so that a linear array of parallel beams is formed. The high degree of parallelism of the etalon faces ensures that the exiting beams are all parallel. These multiple parallel beams are then reflected simultaneously from the sample surface and measured with a CCD camera. The objective lens is used to focus

the beams directly onto the CCD array so that no camera lens is necessary. Typically, five beams can be imaged on the CCD array simulataneously.

The use of multiple beams has several beneficial features for *in situ* measurement. First of all, the optics are very simple. The spatial filter and objective lens can be aligned before mounting on the deposition system and generally require only minimal subsequent alignment. Because a CCD camera is used, the reflected spots are fully imaged and can be viewed on a television monitor for focusing of the objective lens. In addition, because the CCD array has a relatively large active area, if the spots move due to sample motion (for instance during heating) this does not generally require realignment of the camera.

Simultaneous measurement of the multiple spots and no beam scanning make the system inherently less sensitive to sample vibration than the scanning mirror technique. Since all the laser spots move together, noise due to position changes or tilt of the sample do not appear as changes in the curvature. A quantitative representation of this is shown in figure 2. The sample in this run was unconstrained (held by gravity) and would sometimes exhibit a rocking motion, possibly driven by vibrations in the vacuum pumps used on the MBE system. In figure 2a, the variation in time of one of the spot centroids is shown; the excursions correspond to an RMS noise of 4.3 pixels. However the variation in time of the difference between the centroid of this spot and the spot adjacent to it (separated by approximately 120 pixels) is much smaller. Shown in figure 2b, the spacing between the centroids has an RMS deviation of only 0.09 pixels. So even though the positions of the spots may not be stable, the difference between the spots is much less sensitive to vibration.

2-DIMENSIONAL CURVATURE PROFILES

From the relative deflection of adjacent beams, we are able to determine the profile of the curvature across the sample. This is an advantage over the measurements using a beam splitter where only a single beam spacing is obtained. By using a pair of reflective optics oriented orthogonally to the laser beam, we are able to produce a two-dimensional grid of spots on the sample to obtain a two-dimensional curvature profile simultaneously. The results of this technique are shown in figure 3. The sample configuration is shown in figure 3a; the sample is clamped at one end in a cantilever arangement. The spots are incident on the sample at the postions shown in the figure. The reflected spot positions are shown in figure 3b for the as-prepared sample (o) and the sample after growth of 72 angstroms of $Si_{65}Ge_{35}$ (+). The centroids of the two beam profiles have been made to coincide to remove the effect of tilting of the sample. The difference between the spot positions of the flat sample and the curved sample can be related to the surface normal of the sample at the point of impact of the beam. From the surface normals, we can reconstruct a map of how the surface has deformed. In figure 3c, we show an image of the surface after the SiGe alloy growth. Note that the curvature is significantly larger along the unconstrained x-axis than along the y-axis where the clamp prevented the wafer from curving. Also note the difference in scales of the z-axis relative to the in-plane x- and y-axis. The maximum vertical deflection of the surface is less than 0.3 microns.

IN SITU MEASUREMENTS OF STRESS EVOLUTION

We have used the in situ wafer curvature technique for measuring the evolution of stress during growth of Si_xGe_{1-x} alloys on Si(001) substrates. An example of the stress measurement is shown in figure 4 where the evolution of the product of film stress (σ) and thickness (h) during

growth is demonstrated. The three distinct regions of behavior observed during growth are discussed below.

Stress Offset

In the early stages of growth (figure 4a, 0 - 10 Å), the stress increases much more slowly than expected for a strained epitaxial film. We attribute this behavior to segregation of the Ge to the surface during the early stages of growth. After a Ge rich surface layer is formed, the film grows at the nominal composition determined by the growth fluxes. The Ge-rich layer remains on the surface during subsequent growth, presumably by exchanging places with adatoms arriving from the deposition flux. This interpretation is supported by earlier work [9,10] and is also consistent with our measurements of the offset dependence on alloy composition. For decreasing Ge fraction in the film, the offset before the linear elastic regime begin increases since it takes longer to form a surface layer. We also find that growing pure Si after the growth of a SiGe layer results in increasing compressive stress as the surface Ge is re-incorporated into the Si layer. Without the presence of Ge on the surface, the growth of Si would not lead to additional strain since the films are fully pseudomorphic.

Two other possible explanations for this behavior, interface stress and surface morphology, have also been considered. Although interfacial stress can contribute to wafer curvature, it is probably not the dominant source of the offest in figure 4a since the offset is much longer than the time it takes to deposit one monolayer. Alternatively, if the surface is being covered with small islands, it is possible for the islands to be partially strain relaxed without being dislocated. However, simultaneous RHEED (reflection high energy electron diffraction) meaurements of the surface morphology during growth indicate that the surface does not develop sufficient roughness to enable significant relaxation by this mechanism.

Linear Elastic Regime

After the initial offset, σh increases linearly with the film thickness. For thicknesses below the limit for introduction of dislocations, the rate of change of σh is equal to $M(\varepsilon)\varepsilon\, dh/dt$ where ε is the film strain, $M(\varepsilon)$ is the biaxial modulus of the strained alloy film and dh/dt is the growth rate. We have measured $d(\sigma h)/dt$ for different alloy compositions to determine the dependence of $M(\varepsilon)$ on strain. The growth rates and compositions were calibrated using Rutherford backscattering spectrometry (RBS), double crystal X-ray diffraction and X-ray reflectivity. We find that the biaxial modulus can be explained by a simple rule of mixtures over the range of 15 - 60% Ge concentration where the endpoints are the bulk unstrained elastic constants for Si and Ge [11].

Strain Relaxation

As epitaxial films become thicker during growth, they reach a critical thicknes beyond which dislocations can form to decrease the coherency strain energy. The onset of strain relaxation is seen in figure 4b as a decrease in the slope of σh vs. thickness at approximately 400 Å. We have measured the onset of strain relaxation in $Si_{71}Ge_{29}$ alloys grown at temperatures of 450, 550 and 650 ^{o}C [12] .Since the formation of dislocations is thermally activated, the metastable region before the onset of relaxation is larger at lower temperatures. Although strain relaxation kinetics in SiGe alloys have been extensively studied, the laser curvature technique

enables the onset of relaxation and the subsequent kinetics to be measured much more easily than the ex situ techniques that have been previously used.

ACKNOWLEDGEMENTS

We thank Mike Sinclair, Carl Seager and R.C. Cammarata for useful discussions. This work was performed at Sandia National Laboratories and supported by the U.S. Dept. of Energy under contract DE-AC04-94AL85000.

REFERENCES

1. M.F. Doerner, W.D. Nix, CRC Crit. Rev. in Solid State and Mater. Sci. **14**, 225 (1988).

2. P. Flinn, Gardner and Nix. IEEE Trans. Elec. Dev. **ED-34**, 689 (1987).

3. C.A. Volkert, J. Appl. Phys. **70**, 3521 (1991).

4. J.A. Ruud, A. Witvrouw and F.A. Spaepen, J. Appl. Phys **74**, 2517 (1993).

5. A.L. Shull, H.G. Zolla and F.A. Spaepen, Mat. Res. Soc. Symp. Proc. **356**, 345 (1995).

6. R. Martinez, A. Augustyniak and J.A. Golovcenko, Phys. Rev. Lett. **64**, 1035 (1990).

7. A. Schell-Sorokin and R. Tromp,Phys. Rev. Lett. **64**, 1039 (1990).

8. Geisz et al., J. Appl. Phys. **75**, 1530 (1994)

9. K. Fujita, S. Fukutsu, H. Yaguchi, Y. Shiraki and R. Ito, Appl. Phys. Lett. **59**, 2103 (1991).

10. D.J. Godbey and M.G. Ancona, Appl. Phys. Lett. **61**, 2217 (1992).

11. J.A. Floro and E. Chason, unpublished.

12. J.A. Floro and E. Chason, Mat. Res. Soc. Symp. Proc. 1996 (in press).

FIGURE CAPTIONS

Figure 1. Schematic of system for measurement of wafer curvature using multiple parallel beams.

Figure 2. (a) Measurement of the positional variation in the centroid of one of the beams reflected from the sample. The RMS noise corresponds to 4.3 pixels. (b) Measurement of the variation in the difference between the centroids of adjacent beams reflected from the sample. The RMS noise (0.09 pixels) is reduced by a factor of 40 from the noise in the centroid positions.

Figure 3. Reflection of a 2-dimensional array of parallel beams from the sample provides a 2-dimensional profile of the surface curvature. (a) Schematic of the sample configuration with one end clamped showing where the laser beams intersect the sample. (b) Position of the centroids of the reflected beams for the as-prepared sample (o) and after the growth of 72 Å of a $Si_{65}Ge_{35}$ strained film (+). (c) Profile of the curved sample surface after alloy growth reconstructed from the measured change in the surface normal.

Figure 4. Evolution of σh during the growth of a $Si_{71}Ge_{29}$ alloy shows three distinct regions: initial stress offset, linear elastic and strain relaxation. (a) Early stage growth (0-10 Å) shows an initial period of essentially stress-free growth before the linear increase due to coherency strain. (b) Strain relaxation occurs above the critical thickness for dislocation formation.

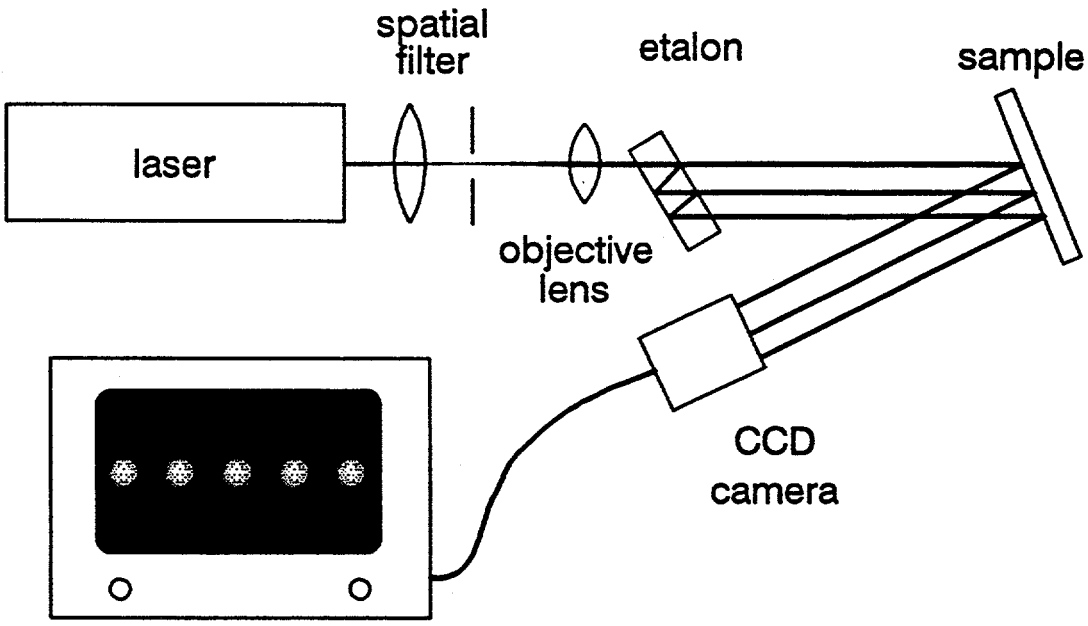

Figure 1.

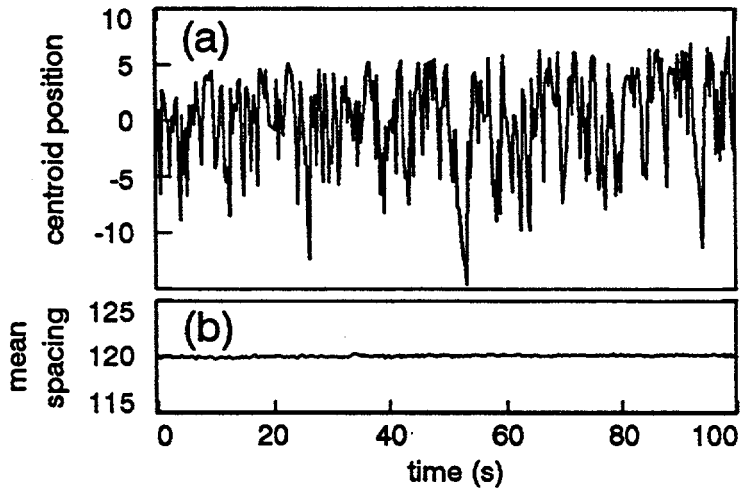

Figure 2.

mrs96\mrs96f12.drw

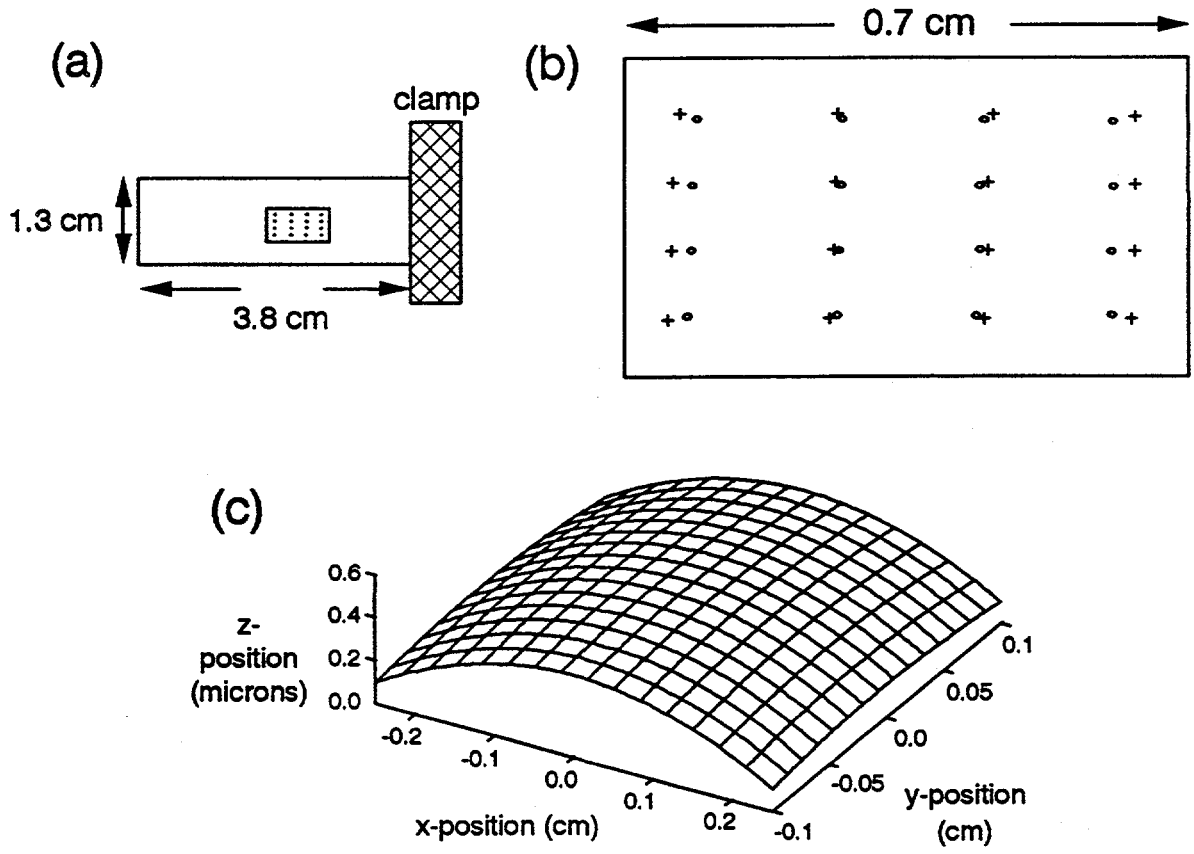

Figure 3

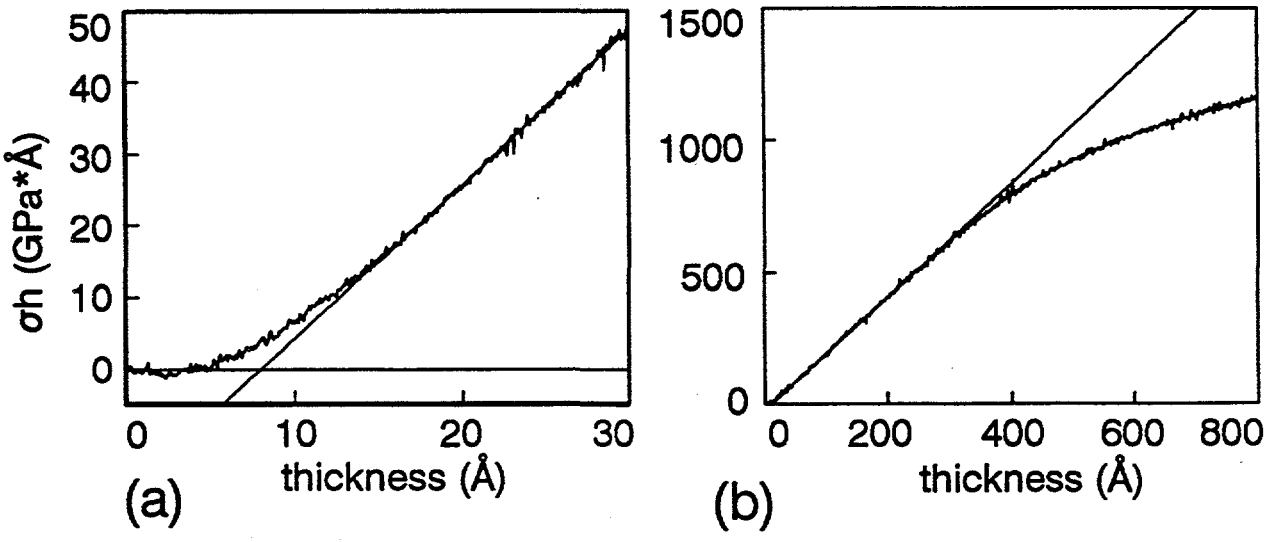

Figure 4

Intentionally Left Blank

Measuring Ge Segregation by Real-Time Stress Monitoring During $Si_{1-x}Ge_x$ Molecular Beam Epitaxy

J. A. Floro and E. Chason

Sandia National Laboratories, Albuquerque, NM 87185-1415

Real-time stress measurements during $Si_{1-x}Ge_x$/Si molecular beam epitaxy are used to dynamically monitor Ge surface segregation. Segregation during alloy growth produces a change in the surface stress that offsets the coherency stress in the pseudomorphic film. We outline a method for analyzing the stress evolution kinetics to determine the alloy composition profile resulting from segregation.

Micro- and opto-electronic applications often demand that interfaces between dissimilar semiconductor layers be well-defined. Interface sharpness will degrade if one of the constituents of a multicomponent semiconductor segregates to the surface during growth. Surface segregation of Ge has been observed to occur during Si_xGe_{1-x}/Si molecular beam epitaxy (MBE) [1-9], presumably driven by the surface energy reduction that results when Si(001) is terminated by a Ge adlayer [2]. The non-uniform film composition profile that results from segregation is difficult to quantify since the length scales involved (< 20 Å) are too small to determine reliably by ex situ depth-profiling techniques. This has hindered our ability to develop an understanding of segregation kinetics. In the $Si_{1-x}Ge_x$/Si system, the only quantitative evaluation of Ge segregation to date comes from measurements of the Ge photoelectron signal from a series of films of varying thickness [5,9].

In this Letter we report real-time stress measurements during $Si_{1-x}Ge_x$ /Si MBE growth. Non-linearities in the stress evolution are determined to result from the segregation process. We outline here the method by which we analyze the time-dependent stress data to determine the Ge composition profile. We emphasize that we do not present here a model of segregation kinetics - we simply demonstrate a means by which these kinetics may be sensitively and efficiently monitored.

Heteroepitaxial $Si_{1-x}Ge_x$ films on Si are in a state of stress due to the difference in lattice parameters between the alloy and the substrate. An additional contribution to the total stress arises from the difference in the *surface* stress between the alloy layer, $F_{SiGe}(t)$, and the Si surface, F_{Si} [10,11]. The film surface stress can be time-dependent if the surface composition or structure evolves during growth. The net biaxial stress (coherency plus surface) produces a curvature of the substrate. The rate of change of the curvature is given by a differential form of Stoney's equation [12,13]:

$$\frac{d\kappa}{dt} = \frac{6}{M_s h_s^2}\left(\sigma(t)\frac{dh_f}{dt} + \frac{d\Delta F(t)}{dt}\right), \qquad (1)$$

where κ is the curvature, σ is the film stress, h_f (h_s) is the film (substrate) thickness, M_s is substrate biaxial modulus, and $\Delta F = F_{SiGe}(t) - F_{si}$ (we assume the surface stress of the SiGe/Si interface is negligible [11]). Following Volkert, we define the "integrated stress" S(t) as [14]

$$S(t) = \frac{M_s h_s^2}{6}\kappa(t) = \int \sigma(t) dh_f + \Delta F(t) \qquad (2)$$

By measuring the instantaneous curvature $\kappa(t)$ in real-time during growth we determine S(t), and thus the evolution of $\sigma(t)$ and $\Delta F(t)$. We measure $\kappa(t)$ using a recently-developed technique called the Multi-beam Optical Stress Sensor (MOSS). MOSS is a laser-deflectometer optimized for real-time stress monitoring during thin film growth. Details may be found in ref. 15.

In the absence of segregation effects, pseudomorphic $Si_{1-x}Ge_x$/Si growth at constant deposition rate and composition would have constant values for σ and ΔF, so that S(t) would vary linearly with time: $S(t) = \sigma R t + \Delta F$, where R is the total deposition rate. We show below that prominent non-linearities in S(t) occur during growth of pseudomorphic alloys at constant rate and Si/Ge flux ratio. We interpret this behavior in terms of surface stress changes associated with Ge surface segregation during growth, which leads to a method for extracting the Ge composition profile from the S(t) data.

$Si_{1-x}Ge_x$ films were grown by MBE (rates: 0.1 - 0.24 Å/s) on both-side-polished Si (001) wafers, 100 μm thick, that were chemically cleaned. The resulting oxide was desorbed in situ at 825°C, followed by growth of a 1000 Å Si buffer at 725°C. A reflection-high-energy-electron-diffraction (RHEED) pattern typical of a smooth, 2x1 reconstructed surface was obtained. The substrate temperature was then reduced to 400°C and allowed to equilibrate for at least one hour before initiating alloy growth. In some instances, a 20 Å Si buffer was grown after the equilibration period, followed immediately by alloy growth. The presence of this buffer did not significantly affect the results.

The integrated stress data for epitaxial $Si_{1-x}Ge_x$/Si films with x = 0.21, 0.3, 0.47 are shown in Fig. 1a. The stress first becomes slightly tensile (positive) prior to exhibiting the expected linear variation in S(t). In Fig. 1b we show the growth of a $Si_{53}Ge_{47}$ film followed by growth of a pure Si cap. Since the alloy layer is pseudomorphic on the Si substrate, the cap should be unstrained and S should be constant during cap growth. Instead, we observe that the compressive stress of the cap gradually increases.

We always observe the initial non-linear behavior shown in Figs. 1a and 1b when growing $Si_{1-x}Ge_x$ on Si. Once in the linear regime, however, interrupting and resuming alloy growth produces no subsequent non-linear behavior. This confirms that effects such as sample heating from the evaporation sources are not responsible for the non-linearities.

The initial non-linearity must arise from a transient time-dependence to the coherency stress $\sigma(t)$ and/or the surface stress $\Delta F(t)$. We rule out stress variation as a result of plastic deformation since the non-linear regime occurs below the equilibrium critical thickness. Also, Ge diffusion into the substrate is insignificant at 400°C. Strain-driven surface-morphological instability could account for the observed behavior. However, RHEED measurements during growth suggest the films remain too smooth to account for the S(t) behavior via this mechanism. We show next that the Ge surface segregation process is consistent with the results of Figs. 1a and 1b.

Surface segregation of Ge during MBE growth is well-known to occur under growth conditions similar to those used here [1,5-9]. Godbey has presented the following phenomenological picture of the segregation process [5]: During alloy growth, arriving Ge atoms will either incorporate onto the alloy lattice, or segregate into a Ge-enriched free surface layer. When growth is initiated, segregation dominates and a Ge-enriched surface layer builds up. This process robs the alloy lattice of Ge, resulting in an underlying denuded zone with a graded composition profile along the growth direction. This corresponds to our initial non-linear S(t) regime. Eventually steady-state is reached wherein a fixed coverage of Ge is segregated on the dynamic growth surface and the film then grows with the composition of the incoming flux. This corresponds to our linear S(t) regime. When a Si cap layer is grown, trapping of the segregated Ge layer into the Si cap occurs [1, 3-8], resulting in further evolution of S(t) as shown in Fig. 1b. The schematic composition profile resulting from behavior is summarized in Fig. 1c. Actual measurements of this profile, especially for the denuded zone, are extremely limited [9].

It is now demonstrated that the non-linear S(t) resulting from the segregation process arises only from changes in the *surface* stress associated with the development of the Ge-enriched surface. While the depth-varying Ge concentration in the denuded zone produces a depth-varying *coherency* stress, curvature-based stress-measuring techniques are *not* sensitive to this variation. In particular, *the curvature does not depend on how the Ge is distributed through the depth of the film*, but only on total amount of Ge deposited (as long as the film surface remains nearly planar and the Ge all resides on lattice-registered sites). For our dynamic experiments, where the Ge deposition rate is kept constant, this implies a linear increase in the curvature with time. To demonstrate this, consider the coherency stress contribution to dS/dt: $\sigma dh_f/dt = M_f x \varepsilon_{Ge} R$, where M_f is the film biaxial modulus, ε_{Ge} is the strain of pure Ge on Si (=0.042), and x is the Ge fraction of the incident flux. Assume that segregation is occurring during growth. Some fraction of the incident Ge flux will

incorporate on the alloy lattice - call this fraction I(t). Assume the remainder, 1-I(t), segregates into a pure Ge layer, fully strained, on the surface. Then

$$\sigma(t)dh_f/dt = M\varepsilon_{Ge}\{x(t)R'(t) + [1-I(t)]R_{Ge}\}, \quad (3)$$

where $x(t) \approx I(t)R_{Ge}/[I(t)R_{Ge}+R_{Si}]$ is the time-dependent Ge concentration incorporated into the alloy layer, and $R'(t) = I(t)R_{Ge}+R_{Si}$ is the net deposition rate into the alloy. Simplifying this expression we get $\sigma dh_f/dt = M\varepsilon_{Ge}R_{Ge}$. Thus, to first order [16], the coherency stress contribution to S(t) is independent of the detailed segregation behavior and depends only on the Ge deposition rate. Since in these experiments R_{Ge} is constant, the non-linearity must arise *only from changes in the surface stress* associated with the formation of the segregated Ge layer .

We now outline the general methodology for extracting the composition profile of the denuded zone from the S(t) data. From Eq. (2) and the considerations just discussed, we have $dS/dt = M\varepsilon_{Ge}R_{Ge} + d\Delta F/dt$. We take $d\Delta F/dt = (d\Delta F/dh_{Ge,s})(dh_{Ge,s}/dt)$, where $h_{Ge,s}(t)$ is the thickness of the segregated Ge layer on the film surface. Further writing $dh_{Ge,s}/dt = R_{Ge}[1-I(t)]$, we get

$$\frac{dS}{dt} = M\varepsilon_{Ge}R_{Ge} + [1 - I(t)]R_{Ge}\frac{d\Delta F}{dh_{Ge,s}} . \quad (4)$$

dS/dt is determined from the time-derivative of our measured data; the constant term $M\varepsilon_{Ge}R_{Ge}$ is known as well. Thus, we may solve Eq. (4) for I(t), the Ge incorporation

fraction, and thus the composition profile, if we can determine $d\Delta F/dh_{Ge,s}$, i.e., how the surface stress depends on the segregated Ge thickness.

We accomplish this by separately growing pure Ge on Si. Fig. 2 shows the integrated stress data for a pseudomorphic Ge film on Si (001). These results are similar to those obtained in a nearly identical experiment performed by Schell-Sorokin and Tromp [17-19], and are consistent with measurements of Ge/Si surface stress by Wu and Lagally [20]

Fig. 2 shows the decomposition of S(t) into the contributions from the known coherency stress and the surface stress, cf. Eq. 2, for Ge/Si growth [21]. The derivative of the $\Delta F(h_{Ge})$ data is the desired function $d\Delta F/dh_{Ge,s}$, if we assume that the surface stress change associated with a given thickness of pure Ge segregated on $Si_{1-x}Ge_x$ is identical to that for the same thickness of pure Ge on Si. We then use the measured $d\Delta F/dh_{Ge,s}$ data in Eq. (4) and solve for I(t). Full details of the solution will be given in a forthcoming paper.

The results of this analysis are shown in Fig. 3 for the films of Fig. 1a. The alloys are significantly non-uniform over the first 15 Å. Thus, for these growth conditions, the chemical interface sharpness between Si and the $Si_{1-x}Ge_x$ alloy is poor, even though the physical interface sharpness is excellent. Such effects could significantly degrade the performance of resonant tunneling structures in which typical well/barrier thicknesses are only tens of angstroms.

The surface Ge coverage is obtained as $h_{Ge,s}(t) = R_{Ge}\int_0^t (1 - I)dt'$. The segregated Ge thickness in steady-state is nearly two monolayers for films with 50% Ge, consistent with recent XPS measurements [9], but in disagreement with a two-state model of segregation that predicts segregation of less than one monolayer of Ge over the entire alloy composition range [6,7].

Finally, we note that our data suggests that reduction of the net strain energy density is a driving force for Ge segregation, since the segregated Ge layer exhibits a tensile surface stress opposing its compressive coherency stress.

The authors thank Glenn Jernigan and Dave Godbey for their willingness to discuss this problem, and Steve Lee and Bob Cammarata for their insights. Our gratitude to Jay Penn for expert assistance with MBE and Steve Casalnuovo for AFM measurements. This work was performed at Sandia National Laboratories and supported by the U. S. Department of Energy under contract DE-AC04-94AL85000.

1. P. C. Zalm, G. F. A. van de Walle, D. J. Gravesteijn, and A. A. van Gorkum, Appl. Phys. Lett. **55**, 2520 (1989).
2. D. E. Jesson, S. J. Pennycook, and J.-M. Baribeau, Phys. Rev. Lett. **66**, 750 (1991).
3. S. Fukatsu, K. Fujita, H. Yaguchi, Y. Shiraki, and R. Ito, Appl. Phys. Lett. **59**, 2103 (1991).
4. K. Fujita, S. Fukatsu, H. Yaguchi, Y. Shiraki, and R. Ito, Appl. Phys. Lett. **59**, 2240 (1991).
5. D. J. Godbey and M. G. Ancona, Appl. Phys. Lett. **61**, 2217 (1992).
6. D. J. Godbey and M. G. Ancona, J. Vac. Sci. Tech. **B 11**, 1120 (1993).
7. D. J. Godbey and M. G. Ancona, J. Vac. Sci. Tech. **B 11**, 1392 (1993).
8. D. J. Godbey, J. V. Lill, J. Deppe, and K. D. Hobart, Appl. Phys. Lett. **65**, 711 (1994).
9. Glenn G. Jernigan, Phillip E. Thompson, and Conrad L. Silvestre, submitted to Appl. Phys. Lett.
10. R. C. Cammarata, Progress in Surf. Sci. **46**, 1 (1994).
11. R. C. Cammarata and K. Sieradzki, J. Elec. Mater. 20, 815 (1991).
12. G. G. Stoney, Proc. Roy. Soc. **A82**, 172 (1909).
13. Mary F.Doerner and William D. Nix, CRC Crit. Rev. in Sol. St. Mat. Sci. **14**, 225 (1988).
14. C. A. Volkert, J. Appl. Phys. **70**, 3521 (1991).
15. J. A. Floro and E. Chason, Mater. Res. Soc. Symp. Proc. **406**, 491 (1996).
16. We have ignored the concentration dependence of the biaxial modulus. Also, the Ge fraction is properly given by the ratio of the deposition fluxes rather than the rates. These approximations produce less than 10% error.
17. A. J. Schell-Sorokin and R. M. Tromp, Phys. Rev. Lett. **64**, 1030 (1990).
18. A. J. Schell-Sorokin and R. M. Tromp, Surf. Sci. **319**, 110 (1994).

19. The initial tensile regime observed here arises when $d\Delta F(0)/dt > M\varepsilon_{Ge}R_{Ge}$. No tensile regime was reported in refs. 17 and 18, where higher growth temperatures were used.

20. Fang Wu and M. G. Lagally, Phys. Rev. Lett. **75**, 2534 (1995).

21. Note that our definition of surface stress differs from that in refs. 17, 18, and 20, which implicitly incorporate the lattice coherency stress into a net "surface stress".

Figure 1. (a) Integrated stress data for $Si_{1-x}Ge_x$ films grown at 400°C, 0.2 Å/s. (b) S(h(t)) for $Si_{53}Ge_{47}$ growth, followed by deposition of a pure Si cap layer. (c) Schematic Ge composition profile, consistent with the data in (b), that arises from dynamic Ge surface segregation. The residual surface spike of Ge is not shown.

Figure 2. Integrated stress data for growth of pure Ge on Si (001) at 400°C, 0.05 Å/s. The contributions to S(t) from the coherency stress and the surface stress change, ΔF, are also shown.

Figure 3. The Ge composition profile of the denuded zone derived from an analysis of the integrated stress data of Fig. 1a.

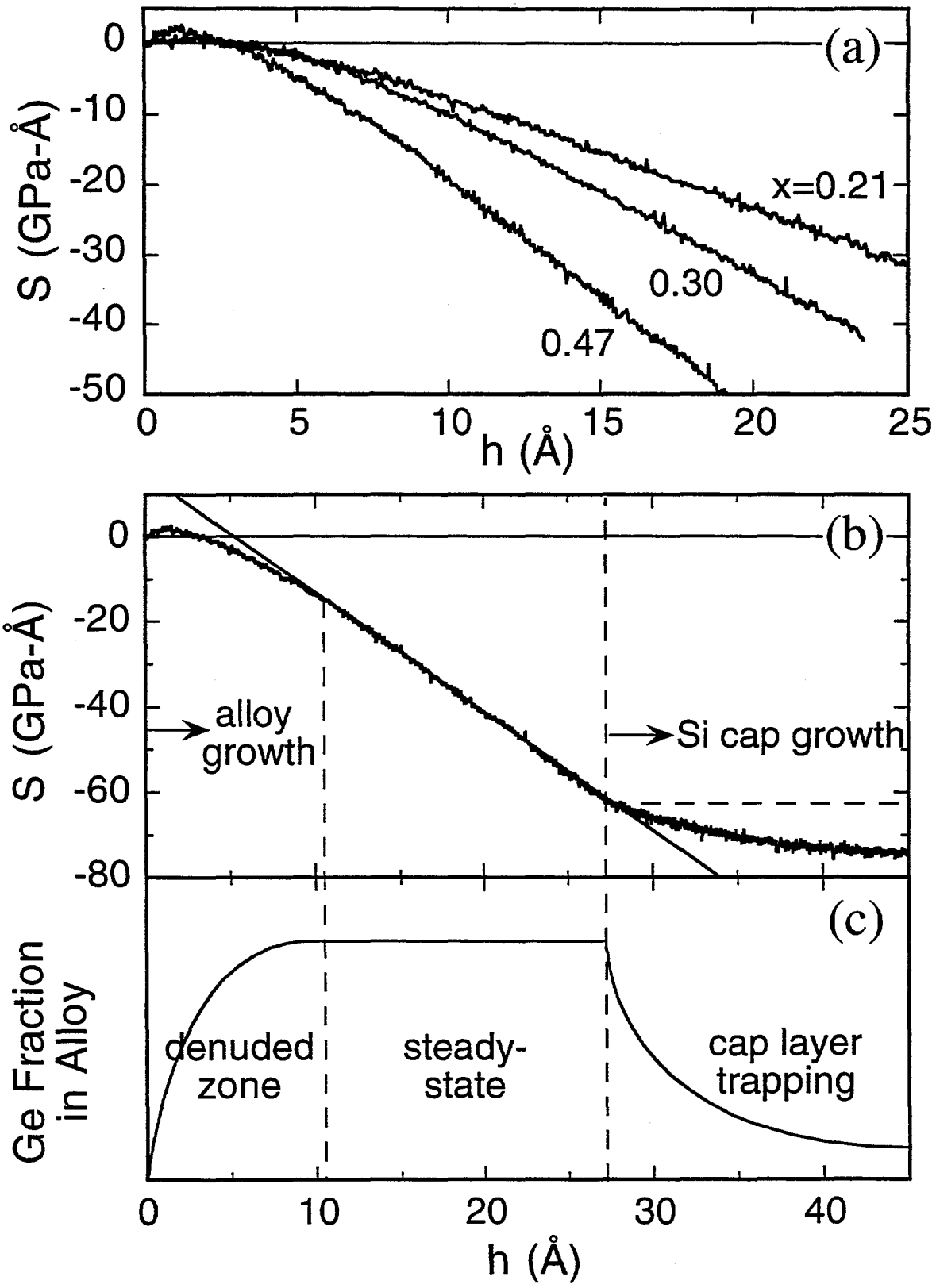
(a)
S (GPa-Å)
0
-10
-20
-30
-40
-50
x=0.21
0.30
0.47
0
5
10
15
20
25
h (Å)
(b)
S (GPa-Å)
0
-20
-40
-60
-80
alloy growth
Si cap growth
(c)
Ge Fraction in Alloy
denuded zone
steady-state
cap layer trapping
0
10
20
30
40
h (Å)

Figure 1

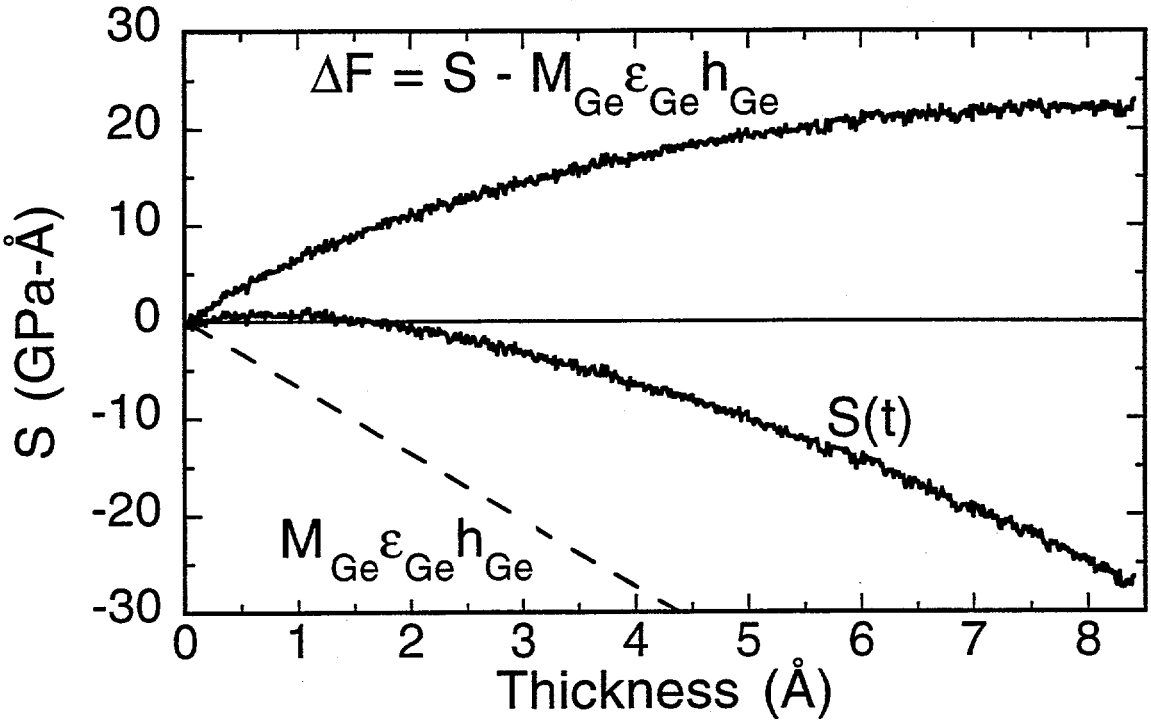
ΔF = S - M_Ge ε_Ge h_Ge
S(t)
M_Ge ε_Ge h_Ge
S (GPa-Å)
Thickness (Å)
30
20
10
0
-10
-20
-30
0
1
2
3
4
5
6
7
8

Figure 2

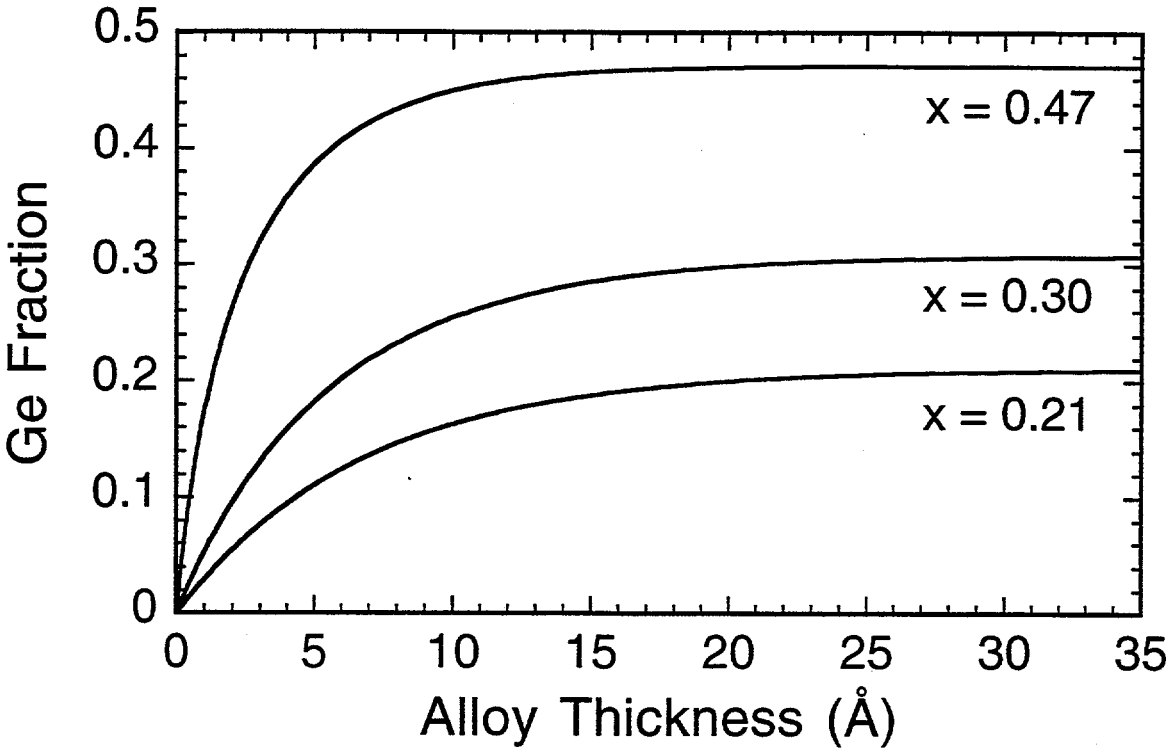
0.5
0.4
0.3
0.2
0.1
0
Ge Fraction
x = 0.47
x = 0.30
x = 0.21
0
5
10
15
20
25
30
35
Alloy Thickness (Å)

Figure 3

DISTRIBUTION:

1	MS-0601	J. S. Nelson, 1113
1	MS-0601	J. L. Reno, 1113
1	MS-0601	J. Tsao, 1126
1	MS-0603	P. E. Esherick, 1314
1	MS-0603	J. F. Klem, 1314
6	MS-1415	E. Chason, 1415
1	MS-1415	J. A. Floro, 1415
1	MS-1415	W. B. Gauster, 1415
2	MS-0619	Review & Approval Desk, 12690 (for DOE/OSTI)
1	MS-0688	LDRD Office, 4523
5	MS-0899	Technical Library, 4414
1	MS-9018	Central Technical Files, 8940-2